Scientific Paper

Solution Mechanisms for Li_2O in Sc_2O_3, Y_2O_3 and La_2O_3

Alexander Chroneos[a,b] and Gerdjan Busker[b]

[a] *Institute of Microelectronics, NCSR Demokritos, Aghia Paraskevi 15310, Greece.*
E-mail: chroneos@imel.demokritos.gr
[b] *Department of Materials, Imperial College, London SW7 2BP, United Kingdom*

Received 12-05-2005

Abstract

Solution mechanisms in bixbyite are studied using atomistic simulation techniques. Defect reactions for the solution of Li^+ ions and the co-solution of Li^+ with A^{2+} ions in Sc_2O_3, Y_2O_3 and La_2O_3 are considered. The co-solution of Li^+ with E^{4+} ions in Y_2O_3 is assessed. Sc_2O_3, Y_2O_3 and La_2O_3 in their bixbyite form are chosen to enhance the ability to compare the effect of the lattice parameter on the solution properties. Both single isolated impurities and defect clusters are considered, the defect clusters are proved to be energetically favourable.

Key words: oxides, lithium, atomistic simulation, migration

Introduction

Rare-earth oxides such as La_2O_3 are of technological significance as effective catalysts.[1] Their catalytic performance is enhanced by alkaline-earth dopants that increase the oxygen defect concentration and mobility.[1] The incorporation of lithium ions is of potential technological importance in nanocrystalline Y_2O_3:Eu powders.[2] Recent experimental studies verify that co-doping modifies the crystallinity of nanoparticles and subsequently their luminescent properties particularly in the case of Li^+ doped Y_2O_3:Eu.[2] Zirconium doped lithium yttrate is a potential solid electrolyte for high temperature lithium sensors.[3]

Ion size is critically important on the thermodynamics and kinetics of physical processes. In ionic materials it is harder to accommodate a large ion at a lattice site previously occupied by a smaller ion. When a small ion is accommodated at a relatively large site the resulting lattice strain acts to reduce the migration activation energy. The advantage when considering a series of dopants is that one need only concentrate on comparative energies rather than the absolute predicted energetics. This is similar to a number of studies of ion size effects in ionic materials.[4–6] The same argument is valid when considering the doping of host lattices with the same crystal structure but with different lattice parameters. This is a systematic study of the effect of doping and defect cluster formation in three materials exhibiting the bixbyite crystal structure but with different lattice parameters. Sc_2O_3, Y_2O_3 and La_2O_3 host materials are doped with a range of aliovalent cations and the results are analyzed as a function of cation radius. The purpose is to determine if the solution and charge compensation mechanisms change with lattice parameter and if it is possible to identify a trend.

In this study calculations were performed using the CASCADE[7] code. CASCADE requires manual set up of the crystal structure, whereas accuracy depends on the precise fitting of the potential parameters.

Crystallography

Sc_2O_3, Y_2O_3 and La_2O_3 exhibit the cubic bixbyite structure (space group Ia3) with lattice parameters of 9.849Å[8], 10.604Å[9] and 11.392Å[9] respectively. The bixbyite structure can accommodate interstitial ions at three distinct sites: the 8b position, the 16c (x=1/8) position and the 24d (x=–1/4) position.

Computational Method

Perfect Lattice

Before simulating the effect of dopants in host materials it is necessary to simulate the properties of the perfect lattice. The perfect lattice is generated by assigning ions to a unit cell which is repeated through space by the application of periodic boundary conditions as described by the crystallographic lattice vectors. Thermodynamically it is a constant pressure calculation as allowing the ions in the unit cell and the lattice vectors to relax to zero strain minimizes the total energy of the system.

Simulation Technique

The simulation technique is based upon a description of the lattice in terms of effective potentials.

The crystal lattice is partitioned into two regions and an interfacial region. In region I interactions are calculated explicitly and all ions are relaxed to zero force. The Newton-Raphson minimization procedure was applied and the first and second derivatives of the energy with respect to strain were calculated. The interactions consist of long-range Coulombic forces and short-range forces. The Coulombic forces are summed using Ewald's method, whereas the short-range forces were modeled using parameterized pair potentials.[5] In region II the Mott-Littleton approximation is applied.[10] In the interfacial region IIa ion displacements are determined with the Mott-Littleton approximation but interactions with ions in region I are calculated by explicit summation. The simulation commences with a perfect lattice calculation where the total energy of the lattice is minimized with respect to the unit cell lattice vectors and the positions of the ions within the unit cell. In the relaxed lattice the region I-II partition is defined and the isolated defect or defect cluster is introduced into the perfect lattice. The lattice is relaxed around the defect as energy minimization proceeds.

It is important to select large enough region sizes so as no significant change in defect formation energy occurs if the region sizes are increased further. In these calculations region I has a radius of 10Å and region IIa extends the radius out to about 30Å.

Calculation of Forces

This study is based on the classical Born model[11] description of the lattice. The short-range energy terms are approximated, by using parameterized pair potentials of the Buckingham form. The interaction energy $S(r_{ij})$ between ion pairs, i and j, is given by

$$S(r_{ij}) = A_{ij} \exp\left(-\frac{r_{ij}}{\rho_{ij}}\right) - \frac{C_{ij}}{r_{ij}^6}$$

where r_{ij} is the separation between ions i and j, A_{ij}, ρ_{ij} and C_{ij} are the potential parameters specific to ions i and j. The parameter values were derived by simultaneously fitting to the relevant crystal properties of a variety of oxides.[12–16] The short-range interatomic potential parameters account for the electron cloud overlap and the dispersion interactions (Table 1).

The Dick and Overhauser shell model was used to describe the ionic polarization effects.[17] In the shell model electronic polarization is described by the displacement of a mass-less charged shell connected to a massive charged core by an isotropic harmonic spring of force constant k [eV Å^{-2}]. The shell model parameters are given in Table 2.

Migration Energy Calculation

The static atomistic simulation code CASCADE was applied to predict defect energies of intermediate steps in migration mechanisms. In bixbyite activated migration mechanisms consist of sequential jumps of the migrating ions between interstitial sites. The activation energy for migration is the difference between the energy of the system when the migrating ion is at the saddle point and the energy of the ion at equilibrium. The saddle point energy is calculated by introducing a fixed lithium ion at the saddle point location and then relaxing the surrounding lattice. The evaluation of the potential energy surface both parallel and perpendicular to the diffusion path is necessary to identify the configuration of the diffusion path.

Table 1. Buckingham interatomic potential parameters.[12–16]

Interaction	A (eV)	ρ (Å^{-1})	C (eV Å^{-6})
O^{2-} - O^{2-}	9547.96	0.21916	32.0
Li^{1+} - O^{2-}	828.01	0.2793	0.0
Mg^{2+} - O^{2-}	1284.38	0.29969	0.0
Zn^{2+} - O^{2-}	529.7	0.3581	0.0
Cd^{2+} - O^{2-}	951.88	0.34856	13.91
Ca^{2+} - O^{2-}	784.38	0.36356	0.0
Sr^{2+} - O^{2-}	682.17	0.3945	0.0
Ba^{2+} - O^{2-}	905.7	0.3976	0.0
Sc^{3+} - O^{2-}	1575.85	0.3211	0.0
Y^{3+} - O^{2-}	1766.4	0.33849	19.43
La^{3+} - O^{2-}	1968.92	0.346	0.0
Ti^{4+} - O^{2-}	2179.122	0.30384	8.986
Zr^{4+} - O^{2-}	1234.73	0.358	0.0
Ce^{4+} - O^{2-}	1809.68	0.3547	20.4
U^{4+} - O^{2-}	1761.775	0.356421	0.0

Table 2. Shell model parameters.

Ion	Shell charge [e]	k [eV Å^{-2}]
O^{2-}	–2.04	6.30
Cd^{2+}	–0.35	190.00
Ti^{4+}	–0.10	200.00
Ce^{4+}	–0.20	177.84
U^{4+}	–0.10	160.00

Results and discussion

Using the potential model described the predicted elastic properties, dielectric properties and the intrinsic defect reaction energies for Y_2O_3 have been compared in a previous paper.[6] The lattice parameters for all the host materials were reproduced to within 0.1% of the experimental values.[8,9]

Solution Mechanisms

All the reactions in this section concern defects that are far apart so they can be considered as isolated. Furthermore, it is assumed that in the systems considered changes in entropy are small compared to the changes in enthalpy. The most efficient way to dissolve isolated

solid Li_2O into a bixbyite host material is given by the reaction (using Kröger-Vink notation[18])

$$3Li_2O(s) \xrightarrow{M_2O_3} 2Li_M'' + 4Li_i^{\bullet} + M_2O_3(s) \qquad (1)$$

Effective charge compensation is achieved by the incorporation of Li^+ ions in both interstitial and metal positions. Calculations showed that the compensation via intrinsic defects, such us oxygen vacancies, results in extremely high solution energies. Reaction (1) solution energies for Li_2O in Sc_2O_3, Y_2O_3 and La_2O_3 are 4.593eV, 4.355eV and 4.516eV respectively.

In real materials different impurity ions are present. Busker *et al* have calculated the solution energies of equal amounts of AO and EO_2 type oxides in solution in Y_2O_3 assuming that (a) both substitutional cations are spatially isolated and (b) the pairs of cations form neutral defect clusters.[6] In this study the co-solution of Li_2O with monoxides in Sc_2O_3, Y_2O_3 and La_2O_3 is considered. Reaction (2) describes the co-solution of Li_2O with monoxides. Divalent ions are used for the charge compensation of Li^+ interstitials.

$$\frac{1}{2}Li_2O(s) + AO(s) \xrightarrow{M_2O_3} A_M' + Li_i^{\bullet} + \frac{1}{2}M_2O_3(s) \quad (2)$$

The monoxides used in order of increasing cation radius are MgO, ZnO, CdO, CaO, SrO and BaO. Figure 1 represents the results of Reaction (2) assuming isolated defects. The co-solution energies are presented as a function of the divalent ionic radii.

Finally, tetravalent ions are used for the charge compensation of Li^+ substitutionals in Y_2O_3. The reaction mechanism is

$$\frac{1}{2}Li_2O(s) + 2EO_2(s) \xrightarrow{Y_2O_3} 2E_Y^{\bullet} + Li_Y'' + \frac{3}{2}Y_2O_3(s) \quad (3)$$

The dioxides used are TiO_2, ZrO_2, CeO_2 and UO_2 and the respective co-solution energies for isolated defects were derived. Data shown in Table 3.

Formation of Defect Clusters

As the computational method used is approximate the focus will not be on the absolute predicted energies but on the differences in predicted energies. The aim is to predict the most energetically favorable solution mechanism. The binding energy (BE) of a defect cluster is equal to the sum of the defect energies of the cluster's component point defects, treated as isolated, minus the defect energy of the cluster itself.[5]

$$BE_{cluster} = \left[\sum_{components} E_{defect}\right] - E_{cluster}$$

The physical meaning of a positive binding energy is that the cluster is preferred energetically over its components. The highest binding energy is the most favorable. In reaction (4) the neutral defect cluster pair formed consists of the Li^+ interstitial and its charge compensating substitutional divalent cation in solution in Sc_2O_3, Y_2O_3 and La_2O_3 host materials.

$$A_M' + Li_i^{\bullet} \Rightarrow \left\{A_M' : Li_i^{\bullet}\right\}^{\times} \qquad (4)$$

The binding energies for these clusters are shown in Figure 2. The binding energies are presented as a function of divalent ionic radii.

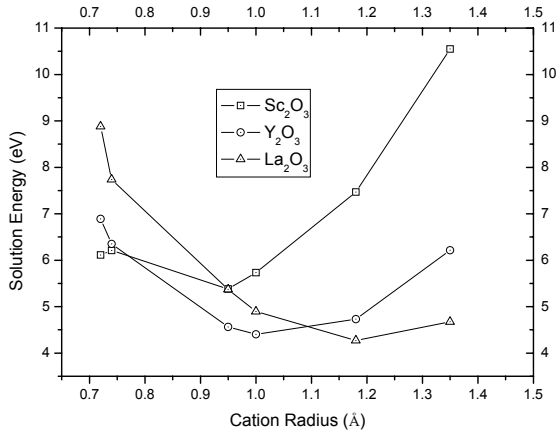

Figure 1. Co-solution of Li_2O with monoxides in Sc_2O_3 Y_2O_3 and La_2O_3 assuming isolated defects (reaction 2). In the x-axis are the values of the divalent cation radii.

The cluster trimer of reaction (5) consists of a Li^+ substitutional and two charge compensating substitutional tetravalent cations.

$$2E_Y^{\bullet} + Li_Y'' \Rightarrow \left\{E_Y^{\bullet} : Li_Y'' : E_Y^{\bullet}\right\}^{\times} \qquad (5)$$

It should be noted that the three defects are in a line with the Li^+ substitutional being in the middle. The most stable geometry occurs when the defects are in nearest neighbour sites. This is because the coulombic attraction is maximized between the defects. Again the dioxides used are TiO_2, ZrO_2, CeO_2 and UO_2 and the respective co-solution energies for the cluster trimmers were derived (Table 3).

Migration of Lithium Ions

Due to symmetry the interstitial sites in the bixbyite structure form two paths. The 8b to 16c path was found to be more energetically favourable than the 16c to 24d path for the migration of lithium ions in Sc_2O_3, Y_2O_3 and La_2O_3 host materials. To verify that the lithium ion follows a straight-line path from 8b to 16c a contour plot was generated representing the plane passing through the saddle point (Figure 3), perpendicular to the migration vector. This contour plot is based on 25 calculations as the lithium ion was positioned in an equidistant 5x5 grid in Y_2O_3. The lowest energy point lies in the middle of the contour plot indicating that the lithium ion followed a straight-line path from interstitial

site 8b to 16c. Equivalent contour plots were generated for Sc_2O_3 and La_2O_3.

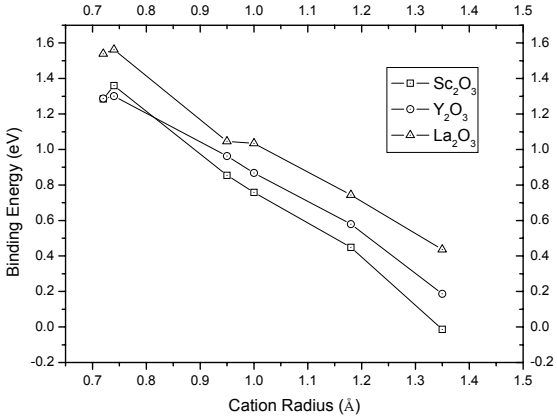

Figure 2. Binding energy for the defect clusters of reaction (4). In the x-axis are the values of the divalent cation radii.

Table 3. Co-solution energies for isolated (Reaction 3) and clustered defects (Reaction 5) consisting of M^{4+} and Li^{1+} substitutionals.

Substitutional ion	$2B_Y^{\bullet} + Li_Y''$	$\{B_Y^{\bullet} : Li_Y'' : B_Y^{\bullet}\}^{\times}$
Ti^{4+}	5.996	3.225
Zr^{4+}	3.544	0.828
Ce^{4+}	4.802	2.148
U^{4+}	5.068	2.417

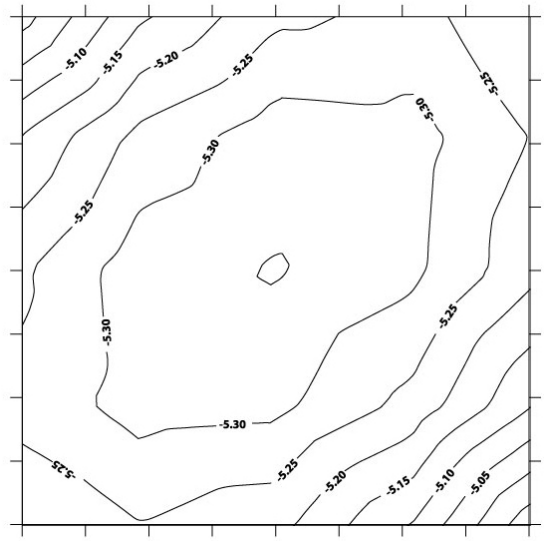

Figure 3. Contour plot of the energy surface for a plane passing through the saddle point perpendicular to the migration vector containing the 16c-8b interstitial sites in Y_2O_3. The contour plot was obtained from positioning the lithium interstitial in 25 mesh points. The contour interval is 0.05eV.

Contour plots parallel to the migration vector containing the 16c-8b-16c interstitial site sequences were generated for the migration of lithium interstitial in Sc_2O_3 (Figure 4), Y_2O_3 and La_2O_3 (Figure 5) host materials. In each of these contour plots the lithium ion was placed in a 21x21 grid and the 16c-8b-16c interstitial sites lie in the diagonal of the plot. The three contour plots are qualitatively similar but the channel connecting the interstitial sites in Sc_2O_3 is comparatively narrow reflecting the lower lattice parameter of this material (Figure 2). The VI coordinate Li^+ ion has an ionic radius of 0.76Å whereas Sc^{3+}, Y^{3+} and La^{3+} have ionic radii 0.745Å, 0.9Å and 1.032Å respectively.[19]

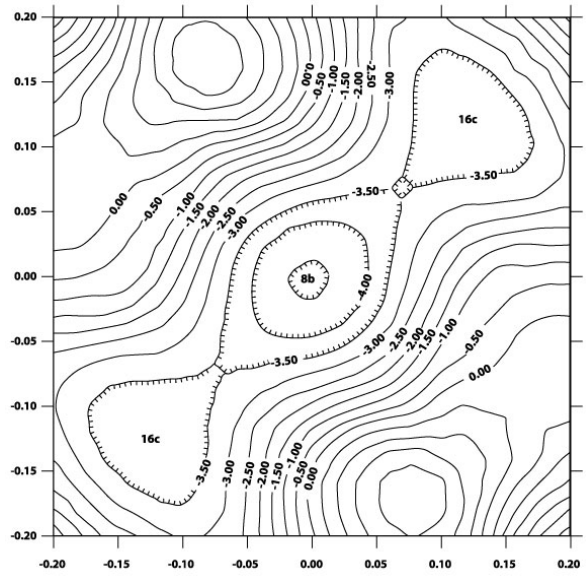

Figure 4. Contour plot of the energy surface for a plane parallel to the migration vector containing the 16c-8b-16c interstitial site sequence in Sc_2O_3. The contour plot was obtained from positioning the lithium interstitial in 441 mesh points. The contour interval is 0.5eV.

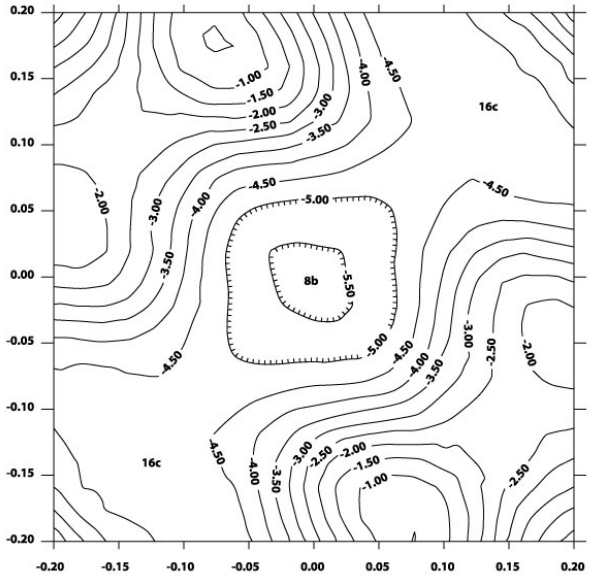

Figure 5. Contour plot of the energy surface for a plane parallel to the migration vector containing the 16c-8b-16c interstitial site sequence in La_2O_3. The contour plot was obtained from positioning the lithium interstitial in 441 mesh points. The contour interval is 0.5eV.

Conclusions

The results suggest that there is a strong dependence of the solution properties on the lattice parameter of the host material. From Figure 1 it can be observed that as the lattice parameter increases the divalent cation radius that results to the minimum co-solution energy increases. To incorporate large divalent cations, such as barium in lattice sites in energetically unfavorable because they have to distort the surrounding lattice.

This effect is particularly important in the lower lattice parameter host oxide Sc_2O_3. From Figure 2 it can be deduced that the variation of the binding energy with respect to the divalent cation radius is qualitatively similar for all three host materials. The formation of defect clusters significantly reduces the co-solution energy of lithium ions with divalent cations. The contour plots highlight that it is more difficult for the Li^+ ion to migrate in the lower lattice parameter bixbyite host lattice. The lowest energy sites are the interstitial sites and the lowest energy path is the straight line connecting the 16c-8b-16c interstitial sites. Through the application of computational approaches it is possible to determine the optimum co-solution combination for host materials of the same crystal structure but different lattice parameters. Atomic scale computer simulation techniques are extremely usefull for screening numerous host oxide materials and can be applied to provide structural and defect formation information. As a fully ionic model was used and the calculations correspond to the dilute limit, the defect energies will be overestimated. Nevertheless, relative energies are very reliable.

Acknowledgements

The authors gratefully acknowledge Robin Grimes of Imperial College for useful conversations.

References

1. M. S. Islam, D. J. Ilett, S. C. Parker, *J. Phys. Chem.* **1994**, *98*, 9637–9641.
2. B. J. Sun, H. W. Song, S. Z. Lu, L. X. Yu, X. B. Zhang, Z. X. Lu, L. M. Yang, J. H. Zhang, X. J. Wang, *J. Rare Earth* **2003**, *21*, 33–36.
3. Y. Zou, A. Petric, *Mater. Res. Bull.* **1993**, *28*, 1169–1175.
4. M. S. Islam, M. Cherry, L. J. Winch, *J. Chem. Soc. Faraday Trans*. **1996**, *92*, 479–482.
5. R. W. Grimes, G. Busker, M. A. McCoy, A. Chroneos, J. A. Kilner, S. P. Chen, *Ber. Bunsen. Phys. Chem.* **1997**, *101*, 1204–1210.
6. G. Busker, A. Chroneos, R. W. Grimes, I. W. Chen, *J. Am. Ceram. Soc.* **1999**, *82*, 1553–1559.
7. M. Leslie, SERC Daresbury Laboratory Report DL/SCI/TM31T, 1982.
8. A. Bartos, K. P. Lieb, M. Uhrmacher, D. Wiarda, *Acta Crys. B* **1993**, *49*, 165–169.
9. R. W. G Wychoff, Crystal Structures. Interscience, New York, 1964.
10. N. F. Mott, M. J. Littleton, *Trans*. *Faraday Soc*. **1938**, *34*, 485.
11. M. Born, K. Huang, Dynamical Theory of Crystal Lattices, Oxford University Press, Oxford, 1954.
12. R. W. Grimes, *J. Am. Cer. Soc*. **1994**, *77*, 378–384.
13. M. A. McCoy, R. W. Grimes, W.E. Lee, *Philos. Mag. A* **1997**, *75*, 833–846.
14. R. W. Grimes, D. J. Binks, A. B. Lidiard, *Philos. Mag. A* **1995**, *72*, 651–668.
15. S. P. Chen, M. Yan, R. W. Grimes, S. Vyas, *Ceramic Trans*. **1997**, *69*, 129–134.
16. M. A. McCoy, R. W. Grimes, W. E. Lee, *Philos. Mag. A* **1997**, *76*, 1187–1201.
17. B. G. Dick, A. W. Overhauser, *Phys. Rev.* **1958**, *112*, 90–103.
18. F. A. Kröger, V. J. Vink, in: F. Seitz, D. Turnbull, (Eds), *Solid State Physics*, vol **3**, Academic Press, New York, 1956.
19. R. D. Shannon, *Acta Crys*., *Sect A: Found. Crystallogr*. **1976**, *32*, 751–753.

Povzetek

Z metodo atomistične simulacije smo raziskovali mehanizem vključevanja ionov v kristale Sc_2O_3, Y_2O_3 in La_2O_3 z kubično biksbitno strukturo. Izbrani sistemi oomogočajo primerjavo med efektom mrežnih parametrov in parametrov raztapljanja oz. vključevanja topljenca. Opazovali smo reakcije nastanke defektov pri vključevanju samo Li^+ , Li^+ in Al^{2+} ter Li^+ in E^{4+} ionov. Ugotovili smo, da ioni v biksbitno strukturo obravnavanih spojin ioni vključujejo tako kot posamezne izolirane nečistoče kot tudi v obliki klastrov defektov. Slednji naj bi bili energijsko ugodnejši.